Electronic Supplementary Material (ESI) for Journal of Materials Chemistry A.

Supporting Information

Eutectic solvent-mediated selective synthesis of Cu-Sb-S-based nanocrystals: Combined experimental and theoretical studies toward highly efficient water splitting

Uma V. Ghorpade[a†], Mahesh P. Suryawanshi[a†], Seung Wook Shin[b, c], Xiaoming Wang[b], Eunae Jo[a], Hyojung Bae[d], KuSung Park[c] Jun-Seok Ha[d], Sanjay S. Kolekar[e*], Jin Hyeok Kim[a**]

[a]Optoelectronics Convergence Research Center and Department of Materials Science and Engineering and, Chonnam National University, 300, Yongbong-Dong, Buk-Gu, Gwangju 61186, South Korea

[b]Department of Physics and Astronomy and Wright Center for Photovoltaic Innovation and Commercialization, University of Toledo, Toledo, Ohio, 43606, USA

[c]Future Agricultural research Division, Water Resource and Environment Research Group, Rural Research Institute, Korea Rural Community Corporation, Ansan-Si, Gyeonggi-do, 15634, Korea.

[d]Department of Chemical Engineering, Chonnam National University, Gwangju 61186, Republic of Korea

[e]Analytical Chemistry and Material Science Research Laboratory, Department of Chemistry, Shivaji University, Kolhapur 416-004, India

Nanocrystals (NCs) synthesis:

For the synthesis of Cu_3SbS_4 NCs, reaction mixture was prepared by stirring and heating the DESs at 80 ^oC in three-neck round bottom flasks along with Cu (II) acetate (3 mmol), Sb (III) acetate (1 mmol) and thioacetamide (4 mmol). The flask was formerly allowed to evacuate and further kept under argon gas throughout the reaction. The reaction temperature was raised up to 120 ^oC and the reaction mixture allowed to age for 15 min. After completion of the reaction, the resulting solution was cooled to room temperature, and ethanol was added to collect NCs, which was then separated by centrifuging. After adequate washing processes, collected material was allowed to dry in vacuum oven.

The above-mentioned experimental procedure was followed for the synthesis of $CuSbS_2$ NCs, except that Cu (II) acetate (1.66 mmol) and Sb (III) acetate (1.66 mmol) and thioacetamide (4.33 mmol) were used and allowed to react at 140 ^oC for 15 min. Similar procedure followed for the synthesis of Cu_3SbS_3 NCs with Cu (II) acetate (3 mmol) and Sb (III) acetate (1 mmol) and thioacetamide (3 mmol) at 130 ^oC for 30 min.

Correspondingly Cu (II) acetate (3 mmol) and Sb (III) acetate (1 mmol) and thioacetamide (3.25 mmol) was allowed to react for 140 ^oC for 15 min. for $Cu_{12}Sb_4S_{13}$ NCs and followed the centrifugation and drying process.

In case Cu_3SbS_4 and $CuSbS_2$ NCs, synthesis parameters, such as reaction temperature (from 80 to 160 ^oC) and time (From 5 min. to 2 hours) were varied for their phase purity. The quantitative percentage yield for optimized Cu_3SbS_4 and $CuSbS_2$ NCs was estimated to be 71 and 83% respectively.

As synthesized Cu_3SbS_4 and $CuSbS_2$ NCs are used for further thin film formation. Toluene dispersion of the corresponding NCs were permitted to spin coat for desired thickness. Afterwards, the films were allowed to bake under controlled air atmosphere on hot plate with facing glass funnel at 300 °C for 15 min. The annealing of the respective film through conventional furnace/rapid thermal annealing process was avoided.

Surface Modification with n-type CdS:

Surface modifications of the Cu_3SbS_4 and $CuSbS_2$ films with n-type CdS layer compounds were performed by using the chemical bath deposition. The procedure of CdS thin film deposition in a hot alkaline medium were adopted from our previously published paper.[1] The reaction mixture was prepared by using 0.2 M $CdSO_4$, 0.84 M ammonia and 1.02 M thiourea solution with controlled pH of 11. Above synthesized nanoparticulate thin films were directly immersed in a reaction bath maintained at 80 ^oC for 8 min. After the deposition, the films were taken out from the reaction bath, rinsed with distilled water and dried in air at room temperature. The CdS modified Cu_3SbS_4 and $CuSbS_2$ absorbers were allow to heat treat at 100 °C for 60 min. in an air atmosphere.

Surface Modification with Pt:

Pt coating on the Cu-Sb-S NCs based thin film and Cu-Sb-S NCs based thin film/CdS was deposited via sputtering for 150 s at room temperature.

Characterization

The structural properties of the NCs were examined by X-ray diffraction (XRD, PANalytical, X'Pert-PRO Netherlands, voltage: 45 kV, current: 40 mA with Ni-filtered Cu-Kα radiation (λ = 1.54056 Å. Raman spectroscopy was recorded using Raman microscope (LabRam HR8000 UV, (Horiba Jobin-Yvon, France), KBSI, Gwangju center). Field emission scanning electron microscopy (FE-SEM, S4800, HITACHI Inc., voltage: 10 kV and current: 20 mA) and high-resolution transmission electron microscopy (HR-TEM, JEOL-3010, acceleration voltage of 300 kV) was used to study the morphology. The elemental mapping images and the compositional ratios were analyzed by an energy-dispersive X-ray spectra (EDS) attached to the FE-SEM (Model Hitachi S 4800, Japan) measured at Korean Basic Science Institute. TEM sampling were carried out by drop casting of NCs dispersed in toluene onto carbon meshed nickel TEM grids (200 meshes, Structure Probe, Inc.). Photoluminescence (PL) spectra were measured on a Horiba-Yvon Fluromax 4 at room temperature. The UV-Visible spectra of each photoelectrode were obtained with Cary 100 (Varian, Mulgrave, Australia) spectrometer at room temperature. Valence band offset (VBO) was measured with ultraviolet photoelectron spectroscopy (UPS) (Thermo VG Scientific, U. K.) with He I (21.22 eV) radiation source. The chemical states of NCs were examined using a HR-X-ray photoelectron spectroscopy (HR-XPS, VG Multi lab 2000, Thermo VG Scientific, UK) with a monochromatic Mg-Kα (1253.6 eV) radiation source. High resolution electrospray ionization mass spectroscopy (ESI-MS) spectra of the DESs were collected from SYNAPT G2 (Waters, U. K. in the positive ion mode using a unit mass resolution microchannel plate (MCP) detector with equipped with a ESI sources assisted by compressed Ar and electrical pumping for the spray solvent. Mass spectra were accumulated over 60 s and scanned over the m/z 100-1000 range. The thermal behavior of the solvent was examined under N_2 atmosphere by thermogravimetry coupled with differential scanning calorimetry (SDT Q600, TA Instruments). The surface structure of the NCs was determined by attenuated total reflection Fourier transformed infrared (FTIR) on a spectrophotometer (PerkinElmer, Frontier-89063) at room temperature. ^1H nuclear magnetic resonance (^1H-NMR) was recorded in deuterium oxide (D_2O, 99.9%, Sigma Aldrich) on a Bruker 500 MHz Avance to elucidate the structural characteristics of the DESs.

Photoelectrochemical (PEC) measurements

The PEC measurements were carried out by following our previously used analysis.[2] The PEC measurements of three-electrode was carried under light illumination using a potentiostat (CHI Instruments, USA) with Pt plate as a counter electrodes, saturated (sat.) Ag/AgCl electrodes as a reference electrode. Nitrogen bubbled mixture of 0.5 M KH_2PO_4/0.5 M Na_2SO_4 aqueous electrolyte of pH ~ 4.3 was used during PEC measurements. A Xe lamp was used as a light source at 150 W with a light intensity of 100 mW/cm^2 with an AM 1.5 filter. Linear sweeps voltammograms (LSVs) under the chopped light on/off illumination were performed at a scan rate of 10 mV/s during the potential sweep. The calibration was performed by using an NREL-certified silicon photodiode.

Gas evolution measurements

An air-tight three-electrode PEC quartz cell reactor with an Ag/AgCl reference electrode, and a Pt wire counter electrode was used for gas chromatography measurements. Photocathodes biased at 0 V_{RHE} in an aqueous solution of 0.5 M H_2SO_4 (pH ~ 0.5) under AM 1.5G simulated sunlight. During irradiation, the headspace gas (50 ml) of the reactor was intermittently sampled and analyzed for H_2 using a gas chromatography (Agilent, 7820A Agilent technology, Santa Clara, California, USA) equipped with a thermal conductivity detector and a molecular sieve 5Å column.

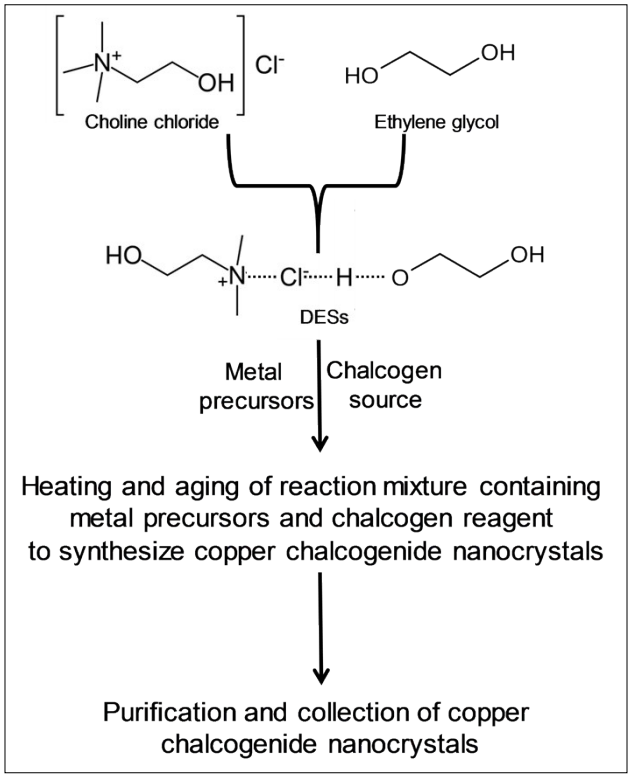

Scheme S1. Reaction pathway for Cu-Sb-S based NCs synthesis process.

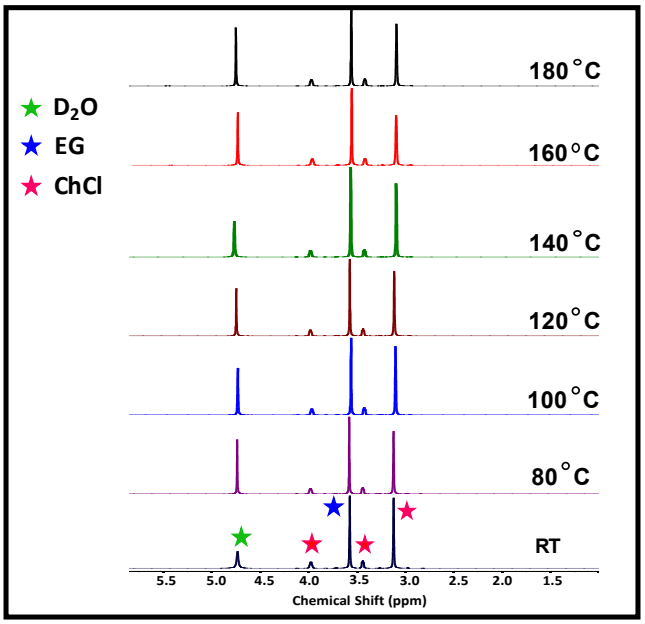

Fig. S1. ^{1}H NMR spectra of without and with heat treated ethaline DES. ^{1}H NMR was taken at room temperature in D_2O.

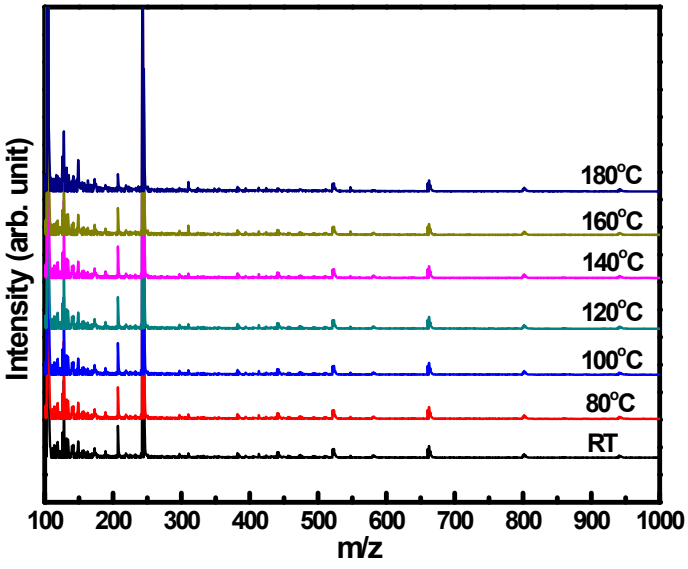

Fig. S2. ESI-MS spectra of ethaline DES without and with heat treatment.

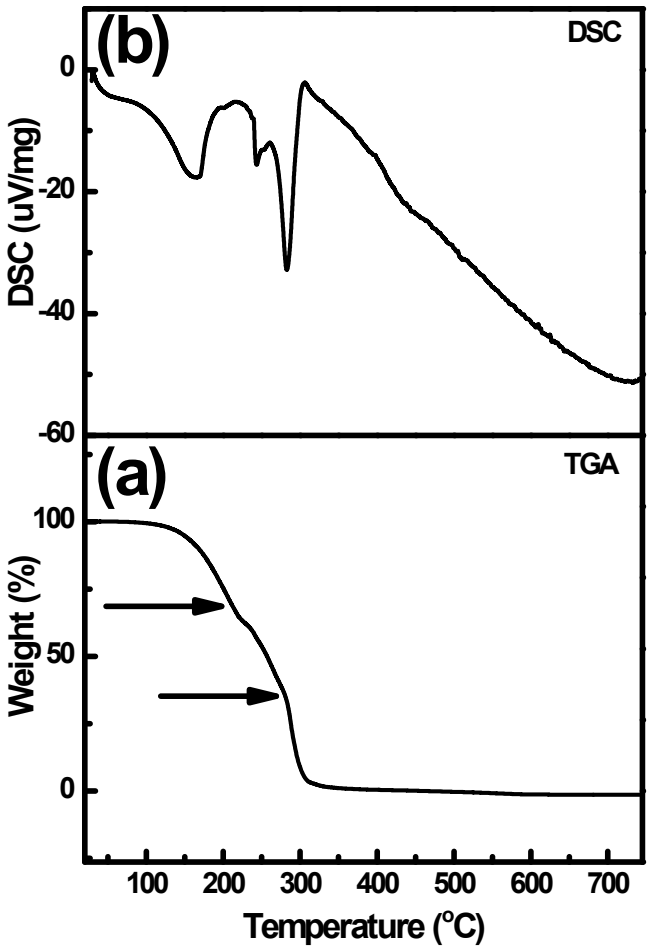

Fig. S3. (a) TGA and (b) DSC analysis of ethaline DES using 1:2 molar of choline chloride and ethylene glycol.

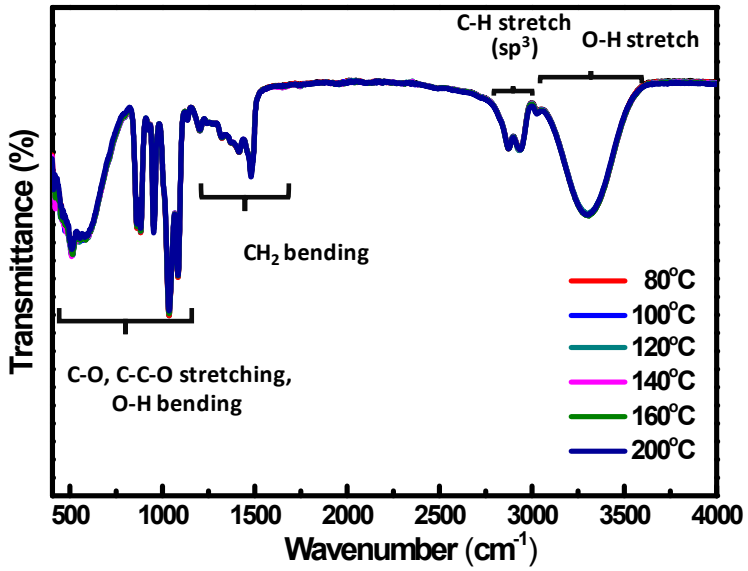

Fig. S4. FTIR spectra of heat treated ethaline DESs

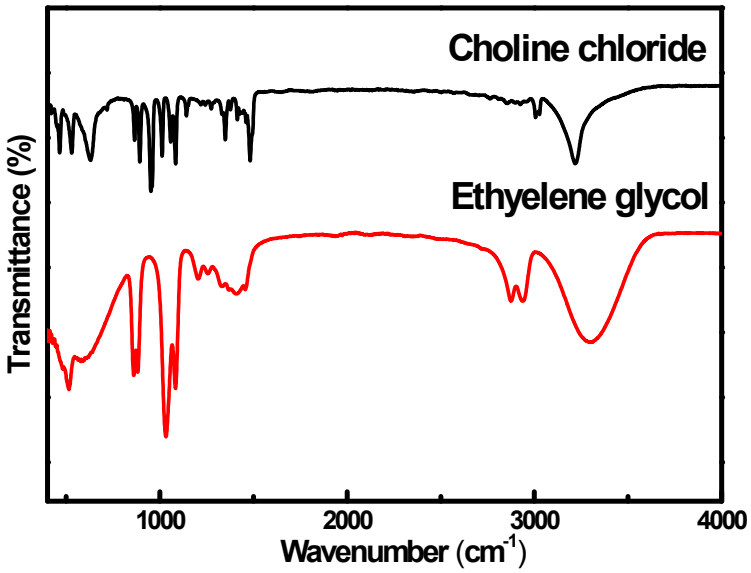

Fig. S5. Room temperature FTIR spectra of choline chloride and ethylene glycol, individual components of the ethaline.

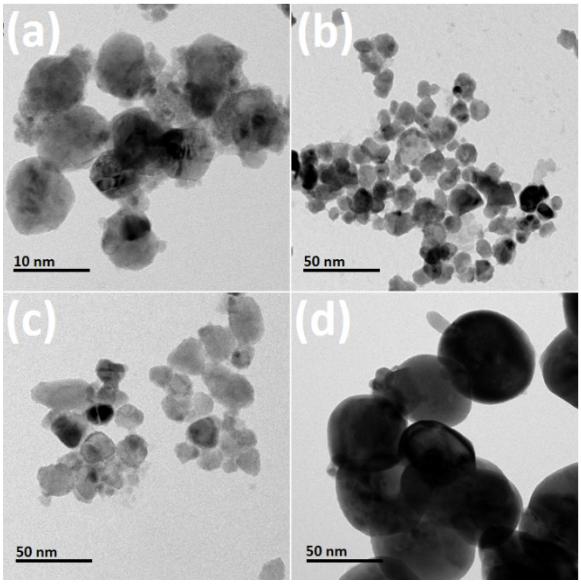

Fig. S6. Low-magnified TEM images of (a) Cu_3SbS_4, (b) $CuSbS_2$, (c) Cu_3SbS_3 and (d) $Cu_{12}Sb_4S_{13}$ NCs.

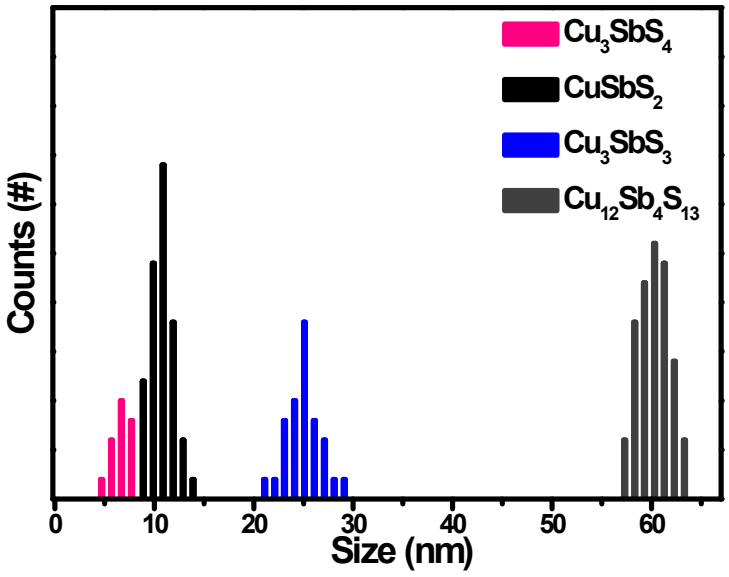

Fig. S7. Size distribution histogram of (a) Cu_3SbS_4, (b) $CuSbS_2$, (c) Cu_3SbS_3 and (d) $Cu_{12}Sb_4S_{13}$ NCs.

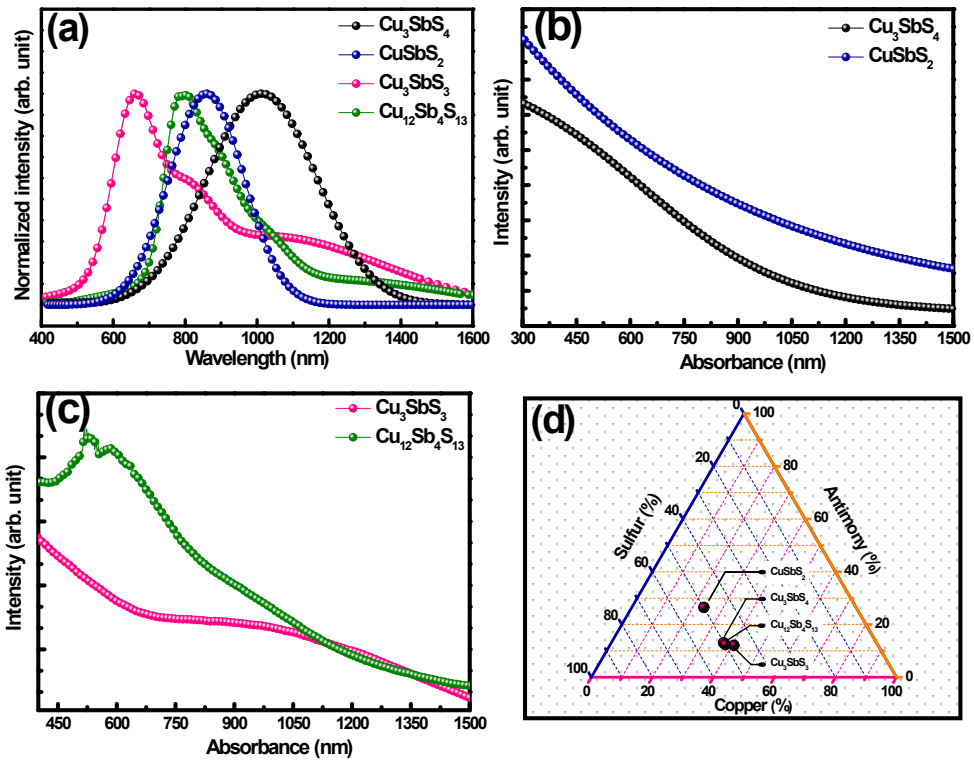

Fig. S8. (a) Normalized PL spectra of Cu_3SbS_4, $CuSbS_2$, Cu_3SbS_3 and $Cu_{12}Sb_4S_{13}$, UV-Vis absorption spectra of (b) Cu_3SbS_4 and $CuSbS_2$ NCs and (c) Cu_3SbS_3 and $Cu_{12}Sb_4S_{13}$ NCs, (d) ternary phase diagram showing compositions of copper, antimony, and sulfur of the four Cu-Sb-S based phases determined using EDS.

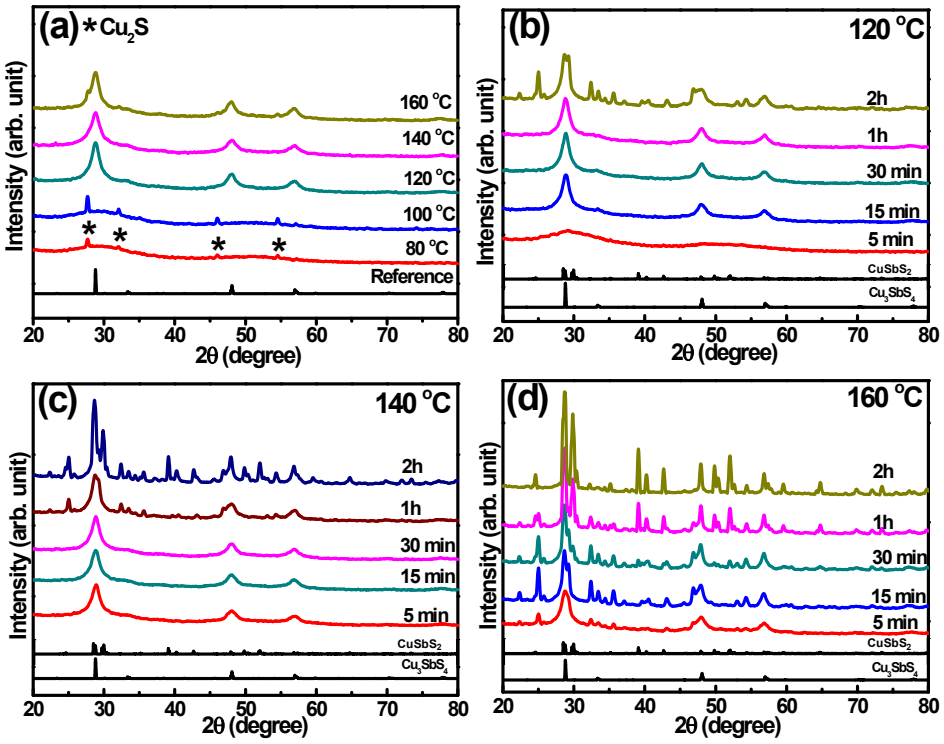

Fig. S9. XRD patterns of Cu_3SbS_4 NCs at (a) different reaction temperature for 15 min. and (b, c, d) at different reaction time at a given temperature. Major diffraction peaks in plot (a) are correspond to Cu_2S phase formation at 80 and 100 °C.

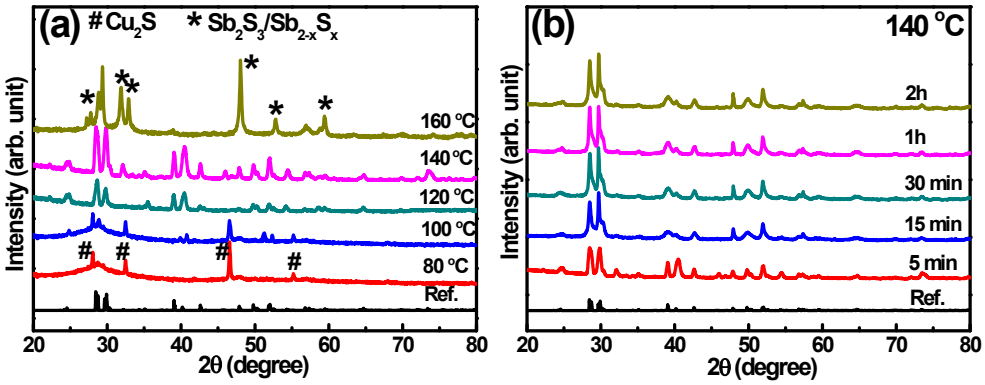

Fig. S10. XRD patterns of $CuSbS_2$ NCs at (a) different reaction temperature for 15 min. and (b) at different reaction time at 140 °C. Major diffraction peaks in plot (a) are correspond to Cu_2S phase formation at 80 and 100 °C.

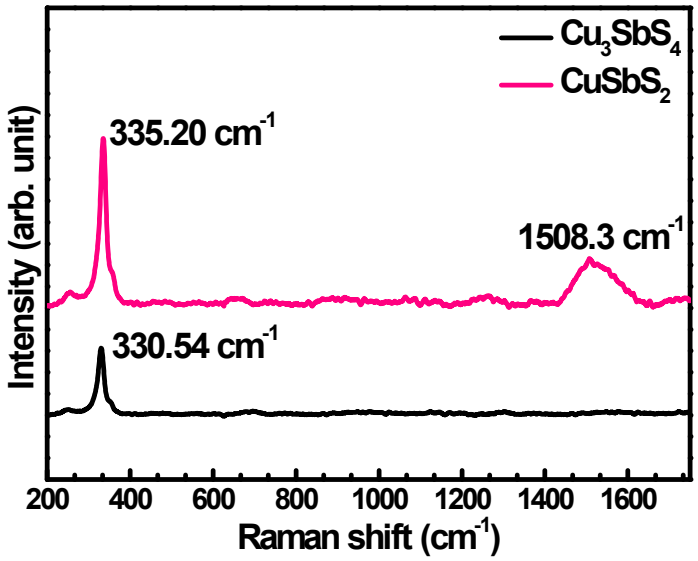

Fig. S11. Raman spectra of a selected Cu_3SbS_4 and $CuSbS_2$ NCs.

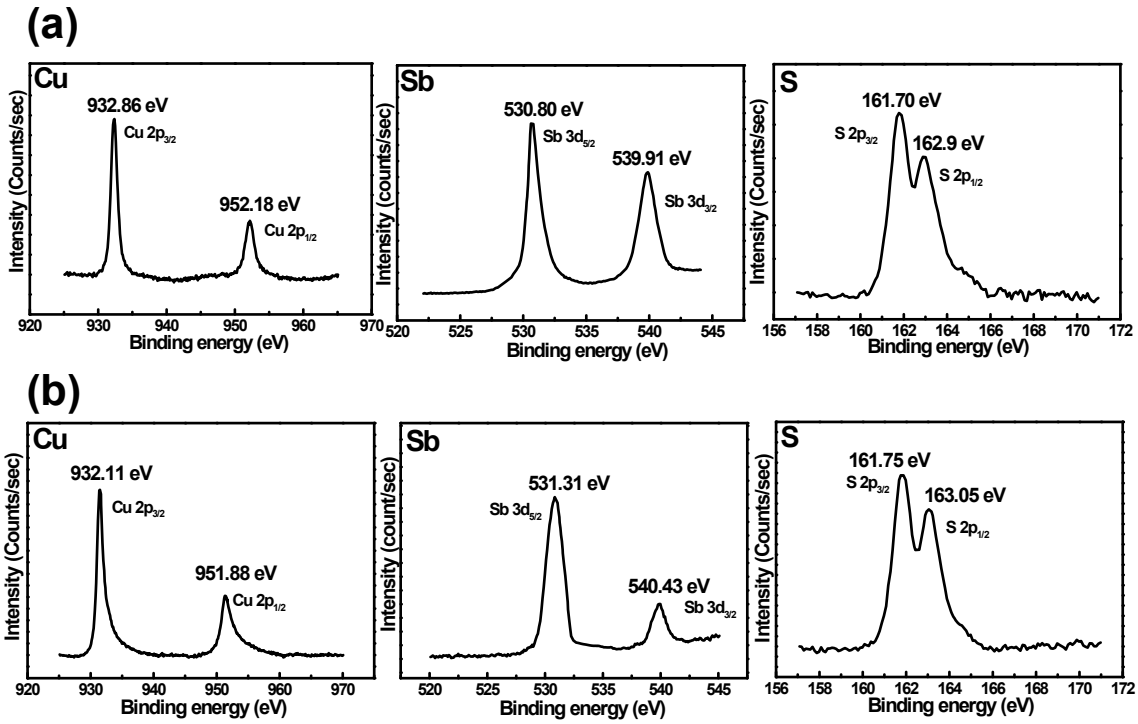

Fig. S12. XPS spectra of an optimized (a) Cu_3SbS_4 and (b) $CuSbS_2$ NCs.

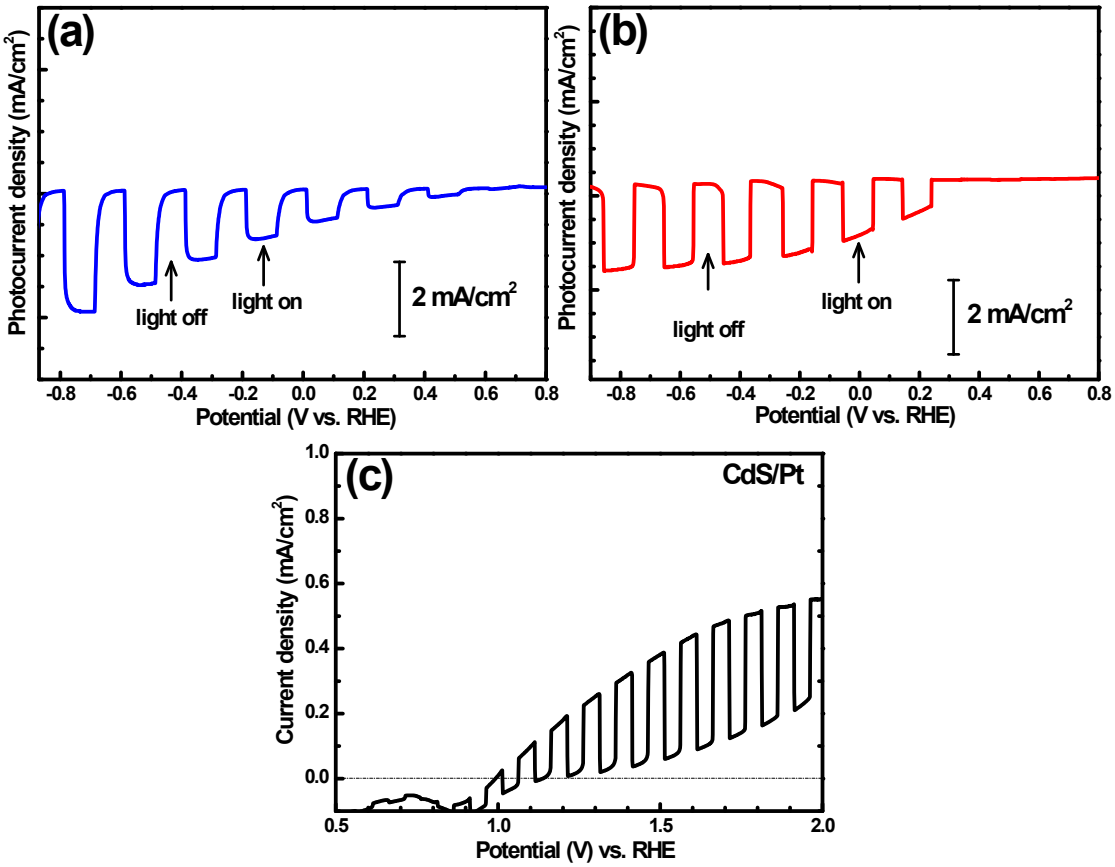

Fig. S13. PEC performance of (a) Cu_3SbS_4/CdS/Pt and of (b) $CuSbS_2$/CdS/Pt photocathode in non-sacrificial reagent of 0.5 M H_2SO_4 and (c) PEC performances of CdS/Pt electrode in 0.5 M KH_2PO_4/0.5 M Na_2SO_4.

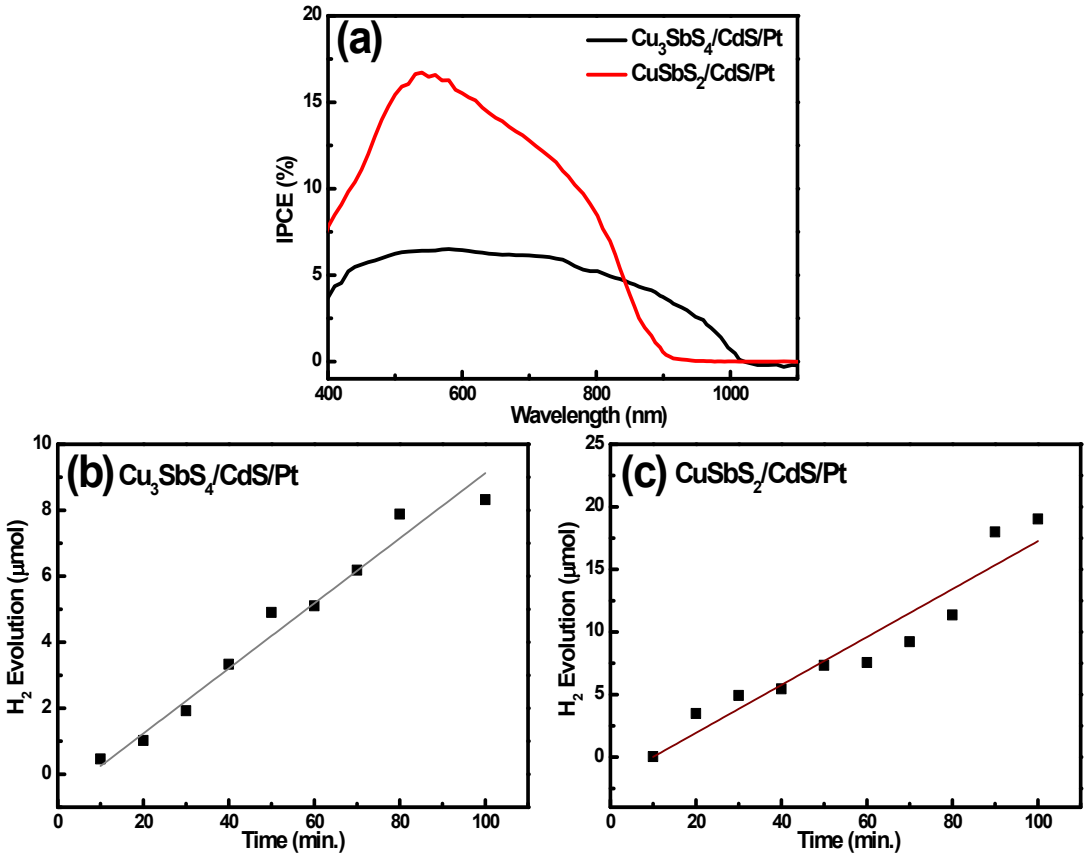

Fig. S14. (a) IPEC and, (b) and (c) H_2 evolution performance of a Cu_3SbS_4/CdS/Pt and $CuSbS_2$/CdS/Pt photocathodes respectively.

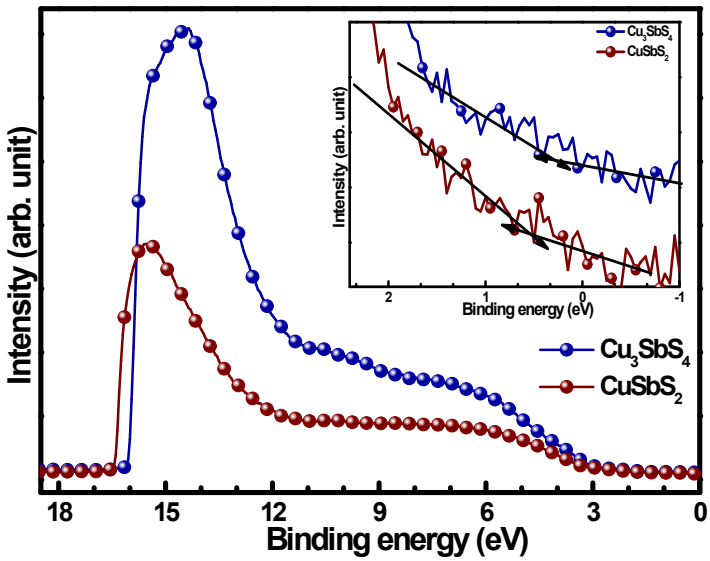

Fig. S15. UPS spectra of Cu_3SbS_4 and $CuSbS_2$ NCs. Inset of Fig. shows the enlarged region of cut-off of the secondary photoelectrons regions with He I excitation energy of 21.22 eV.

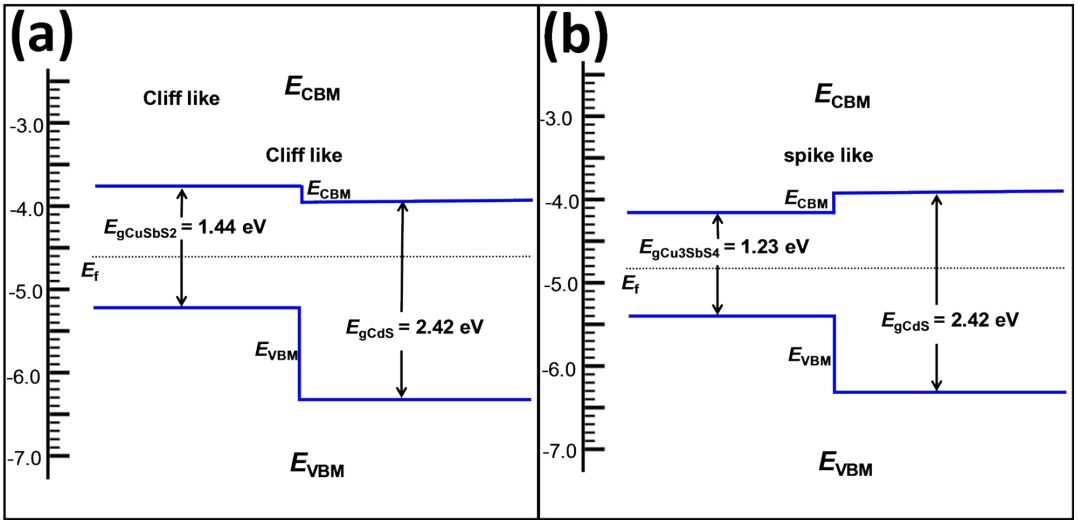

Scheme S2. The band alignment of the a) $CuSbS_2$/CdS and a) Cu_3SbS_4/CdS heterojunction materials.

Table S1. Representative results of the synthesis of different materials by using various DESs.

Name	**Method**	**Size (nm)**	**Shape**	**Application/remark**	**Type of DESs**	**Temp.**	**Ref.**
Ag TF	Electrodeposition	20-80	Nanoporous network	Hydrophilic nature	ChCl-EG	50 °C	S3
ZnO	One pot	60	Twin-cones	--	ChCl–urea	70 °C	S4
Zn TF	Electrodeposition	--	--	Electrochemical Properties	ChCl-EG	30 °C	S5
Au	One pot	17.74	Nanowires	Catalyst	ChCl–urea, ChCl-EG	40 °C	S6
PbS	Hot injection	31, 100~2500	Star shape	--	ChCl–urea	140 °C, 14 min	S7
Pt	Electrodeposition	~200	Nanoflowers	Catalyst	ChCl–urea	80 °C	S8
$NiCl_2$	Ionothermal method	100	Nanosheets	Sodium-ion batteries	ChCl–urea	150 °C, 4 h,	S9
NiO	Ionothermal method	4-6	Nanoflowers	Pseudo-capacitive Electrode	ChCl–urea	150 °C, 40 min	S9
CoFe	Electrodeposition	10-20	Porous Nanosheets	Magnetic adsorbents	ChCl–urea	260 °C, 40-55 min.	S10
Pd	Electrodeposition	223 ± 19	Concave Disdyakis	Shape-controlled Synthesis, catalyst	ChCl–urea	60 °C	S11
Zn Phosph-ate	Hydrothermal	--	Lamellar crystals	photoluminescence and photochromic	ChCl-OA	180 °C for 3 d	S12
Mn_2O_3	One pot heat up	18	Spherical NPs	Paramagnetic behavior	ChCl-EG	140 °C, 2 min	S13
CIGS	One pot electrodeposition	TF	--	TFSC	ChCl–urea	--	S14
CIGS	Electrodeposition	TF	--	TFSCs_7.9%	ChCl–urea	Annealing at 550 °C	S15
CZTS	Co-electrodeposition	TF	--	TFSCs_3.87 %	ChCl–urea	Annealing at 550 °C for 1h	S16
CIGS	Electrodeposition	TF	--	TFSCs_10.1%	ChCl–urea	Annealing at 550 °C for 1h	S17

Where, TF= thin film, ChCl = choline chloride, EG = ethylene glycol, OA= oxalic acid, TFSC = thin film solar cell

Table S2. Viscosities of the commonly used DESs during different materials synthesis used in Table S1.

Type of solvent	Salt ratio	Viscosity (cP)
Reline	Choline chloride: Urea (1:2)	169 (25 ^{0}C)
Ethaline	Choline chloride: Ethylene glycol (1:2)	37 (25 ^{0}C)
Glyceline	Choline chloride: Glycerol (1:2)	259(25 ^{0}C)

REFERENCES

1. C. W. Hong, S. W. Shin, M. P. Suryawanshi, M. G. Gang, J. Heo and J. H. Kim, *ACS appl. Mater. Interfaces*, 2017, **9**, 36733-36744.

2. M. P. Suryawanshi, U. V. Ghorpade, S. W. Shin, M. G. Gang, X. Wang, H. Park, S. H. Kang and J. H. Kim, *ACS Catal.*, 2017, **7**, 8077-8089.

3. C. Gu, X. Xu and J. Tu, *J. Phys. Chem. C*, 2010, **114**, 13614-13619.

4. J.-Y. Dong, Y.-J. Hsu, D. S.-H. Wong and S.-Y. Lu, *J. Phys. Chem. C*, 2010, **114**, 8867-8872.

5. A. H. Whitehead, M. Pölzler and B. Gollas, *J. Electrochem. Soc.*, 2010, **157**, D328-D334.

6. M. Chirea, A. Freitas, B. S. Vasile, C. Ghitulica, C. M. Pereira and F. Silva, *Langmuir*, 2011, **27**, 3906-3913.

7. A. Querejeta-Fernández, J. C. Hernández-Garrido, H. Yang, Y. Zhou, A. Varela, M. Parras, J. J. Calvino-Gámez, J. M. González-Calbet, P. F. Green and N. A. Kotov, *ACS Nano*, 2012, **6**, 3800-3812.

8. L. Wei, Y.-J. Fan, H.-H. Wang, N. Tian, Z.-Y. Zhou and S.-G. Sun, *Electrochim. Acta*, 2012, **76**, 468-474.

9. X. Ge, C. Gu, Y. Lu, X. Wang and J. Tu, *J. Mater. Chem. A*, 2013, **1**, 13454-13461.

10. X. Ge, C. Gu, X. Wang and J. Tu, *J. Colloid Interface Sci.*, 2015, **454**, 134-143.

11. L. Wei, C.-D. Xu, L. Huang, Z.-Y. Zhou, S.-P. Chen and S.-G. Sun, *J. Phys. Chem. C*, 2015, **120**, 15569-15577.

12. P. C. Jhang, N. T. Chuang and S. L. Wang, *Angew. Chem.*, 2010, **122**, 4296-4300.

13. M. Karimi and M. Eshraghi, *J. Alloys Compd.*, 2017, **696**, 171-176.

14. M. Harati, J. Jia, K. Giffard, K. Pellarin, C. Hewson, D. A. Love, W. M. Lau and Z. Ding, *Phys. Chem. Chem. Phys.*, 2010, **12**, 15282-15290.

15. J. C. Malaquias, D. Regesch, P. J. Dale and M. Steichen, *Phys. Chem. Chem. Phys.*, 2014, **16**, 2561-2567.

16. H. Chen, Q. Ye, X. He, J. Ding, Y. Zhang, J. Han, J. Liu, C. Liao, J. Mei and W. Lau, *Green Chem.*, 2014, **16**, 3841-3845.

17. Y. Zhang, J. Han and C. Liao, *J. Electrochem. Soc.*, 2016, **163**, D689-D693.